

Giant spin shift current in two-dimensional altermagnetic multiferroics VOX₂

Yao Yang,¹ Jinxiong Jia,^{1,3} Longjun Xiang,¹ Fuming Xu,^{1,2} and Hao Jin^{1,*}

¹College of Physics and Optoelectronic Engineering, Shenzhen University, Shenzhen 518060, China

²Quantum Science Center of Guangdong-Hongkong-Macao Greater Bay Area (Guangdong), Shenzhen 518045, China

³Department of Physics, and CAS Key Laboratory of Strongly-Coupled Quantum Matter Physics, University of Science and Technology of China, Hefei, Anhui 230026, China

(Dated: March 18, 2025)

Altermagnets represent a novel class of magnetic materials that integrate the advantages of both ferromagnets and antiferromagnets, providing a rich platform for exploring the physical properties of multiferroic materials. Here, we demonstrate that VOX₂ monolayers (X = Cl, Br, I) are two-dimensional ferroelectric altermagnets, as confirmed by symmetry analysis and first-principles calculations. VOI₂ monolayer exhibits a strong magnetoelectric coupling coefficient ($\alpha_S \approx 1.208 \times 10^{-6}$ s/m), with spin splitting in the electronic band structure tunable by both electric and magnetic fields. Additionally, the absence of inversion symmetry in noncentrosymmetric crystals enables significant nonlinear optical effects, such as shift current (SC). The x-direction component of SC component is observed to have an ferroicity-driven switch. Moreover, the σ^{yyy} component exhibits an exceptionally large spin SC of $330.072 \mu\text{A}/\text{V}^2$. These findings highlight the intricate interplay between magnetism and ferroelectricity, offering versatile tunability of electronic and optical properties. VOX₂ monolayers provide a promising platform for advancing two-dimensional multiferroics, paving the way for energy-efficient memory devices, nonlinear optical applications and opto-spintronics.

INTRODUCTION

Magnetoelectric multiferroics are materials that simultaneously exhibit ferromagnetic and ferroelectric properties, with an intrinsic coupling between these two order parameters [1]. The ability to control magnetism using an electric field, or vice versa, holds great potential for applications in low-power electronics, sensors, memory devices, and emerging computing technologies [2–6]. The discovery and development of magnetoelectric multiferroics have unlocked exciting opportunities in materials science and condensed matter physics.

On one hand, due to the intrinsic repulsion between charge polarization and spin polarization, multiferroic materials are inherently rare [7–10]. On the other hand, conventional magnetic materials are typically classified as either ferromagnetic or antiferromagnetic. Compared to ferromagnets, antiferromagnets offer higher information storage density and unique terahertz spin dynamics, enabling magnetic moment reversal on a picosecond timescale [11–14]. However, the weak response of antiferromagnets to external fields and the challenges in controlling their spin order significantly limit their application in multiferroic systems.

Recently, altermagnets have been proposed as a third type of non-relativistic collinear magnetic phase, distinct from both ferromagnets and antiferromagnets [15, 16]. Altermagnets combine the advantages of both ferromagnets and antiferromagnets, exhibiting zero net magnetization while maintaining momentum-dependent spin splitting [17]. It has been experimentally confirmed in materials such as MnTe [18, 19] and CrSb [20, 21]. The discovery of altermagnets not only circumvents the limi-

tations of antiferromagnetic multiferroics but also introduces a new paradigm for magnetoelectric multiferroic materials. The emergence of altermagnets has brought about many novel physical phenomena, such as unique spin currents [22], giant magnetoresistance, tunnel magnetoresistance [23–25], the anomalous Hall effect [26], and the quantum anomalous Hall effect [27].

With the rapid development of two-dimensional (2D) materials, exemplified by graphene, an increasing number of novel layered structures have been explored [28–30]. The advent of 2D materials provides a promising pathway for the miniaturization and integration of electronic components. Thus, achieving the coexistence of ferroelectricity and magnetism in 2D materials has become a significant research direction in the field of magnetoelectric multiferroics. Yang et al. first proposed the concept of sliding ferroelectricity as a means to achieve electric field control of altermagnetism [31]. Zhou et al. further demonstrated the control of altermagnetism via an electric field in antiferroelectric altermagnets, providing experimental validation of magnetoelectric coupling [32]. Despite the advantages of altermagnets, the integration of ferroelectricity into multiferroic systems to control altermagnetism remains underexplored. Further investigations in this field are crucial for advancing next-generation multiferroic materials.

In this work, we propose VOX₂ (X = Cl, Br, I) as two-dimensional ferroelectric altermagnets based on symmetry analysis. First-principles calculations reveal that VOX₂ exhibits an electronic structure with spin splitting and huge magnetoelectric coupling. Further studies indicate that the band splitting can be effectively tuned by electric and magnetic fields. Additionally, the σ^{xxx} component of VOX₂ is tunable via ferroelectric polar-

ization. while the σ^{yyy} component of the VOI₂ monolayer exhibits an exceptionally large spin shift current (SC), This study not only deepens the understanding of magnetoelectric coupling mechanisms in two-dimensional materials but also holds profound implications for the advancement of energy-efficient memory devices, nonlinear optical applications, and opto-spintronic technologies.

CRYSTAL STRUCTURE AND SYMMETRY ANALYSIS

VOI₂ belongs to the van der Waals (vdW) multiferroic family VOX₂ (X = Cl, Br, I) [33]. The VO₂I₄ monolayer forms a two-dimensional octahedral network, where adjacent V atoms share a corner oxygen along the *a* direction and an iodine (I₂) edge along the *b* direction. First-principles calculations predict that the VOI₂ monolayer exhibits both ferroelectricity and ferromagnetism [34], with the V atoms at the center of the octahedra displaced toward the oxygen atoms. This configuration is referred to as the FE-I phase.

Peierls transitions frequently occur in quasi-one-dimensional chain-like structures [35, 36]. The VOI₂ monolayer undergoes a V-V dimerization, leading to a Peierls transition, forming the FE-II phase [37]. This phase belongs to the space group Pmm2 (No. 25), as shown in Fig. 1(a). The two ferroelectric polarization directions ($-P_x$ and P_x) are illustrated in Fig. 1(b), respectively.

The ferroelectric polarization in VOI₂ breaks the \mathcal{PT} symmetry, while the Peierls transition eliminates the $\mathcal{T}\tau$ symmetry. The symmetry operations of the altermagnetic VOI₂ monolayer (collinear antiferromagnetic order along the *x* axis) can be described by spin space groups (SSG), which are given by:

$$\{\mathcal{E}, \mathcal{M}_z\} + \mathcal{R}_S \{\mathcal{M}_y, \mathcal{C}_{2x}\},$$

where the antisymmetric operator \mathcal{R}_S flips the spin, analogous to the relativistic time-reversal symmetry \mathcal{T} . Here, \mathcal{E} represents unitary symmetries, \mathcal{M}_y (\mathcal{M}_z) denotes mirror symmetry about the *y* (*z*) axis, \mathcal{C}_{2x} represents twofold rotation symmetry about the *x* axis, and $\tau_{\frac{1}{2}}$ corresponds to a translation shift of half a lattice period. Both VOCl₂ and VOBr₂ also exhibit altermagnetic phases.

Based on crystal field theory, the V 3*d* orbitals in VOX₂ monolayer under an octahedral environment. VOX₂ has a *d*¹ configuration, where V⁴⁺ hosts a single electron in the *d*_{*xy*} orbital. The spin charge density of VOX₂ monolayer, shown in Fig. S2, reveals a strong *d*_{*xy*} orbital character. The interactions between V-3*d*_{*xy*} orbitals along the *b* axis leads V-V dimers, forming alternating σ bonding and σ^* antibonding states. The exchange interaction along the V-X direction is governed by the competition between two types of exchange mechanisms

[34]: (1) the direct exchange interaction between neighboring V atoms, favoring antiparallel spin alignment, and (2) the superexchange interaction mediated by halogen atoms, promoting parallel spin alignment. The Peierls transition enhances the direct exchange interaction, favoring antiparallel spin arrangements, consistent with the Goodenough-Kanamori-Anderson rule [38]. VOX₂ monolayer exhibits parallel spin alignment along the V-O direction, akin to the FE-I phase [34].

ELECTRONIC STRUCTURE

The ferroelectric polarization and Peierls phase transition break the \mathcal{PT} and $\mathcal{T}\tau_{\frac{1}{2}}$ symmetries. This unique characteristic enables spin splitting at general momentum **k** even in the absence of spin-orbit coupling (SOC). Fig. 1(c) presents the band structure of monolayer VOI₂ along both high-symmetry and general **k** paths. Notably, along high-symmetry **k** paths, the bands exhibit Kramers spin degeneracy, particularly along the X- Γ -Y-S path. However, while the magnitude of spin splitting adheres to the full nonmagnetic crystal symmetry, its sign alternates, ensuring that the material as a whole maintains spin-compensated symmetry [38]. As a result, the net magnetization of the altermagnetic phase of monolayer VOI₂ remains zero, as clearly indicated in the density of states in Fig. S2(c). The detailed spin splitting near the Fermi level for the first valence and conduction bands, with maximum spin splittings of 12.26 meV and 37.68 meV, respectively. The spin splitting energy is comparable to that of SnS₂/MnPSe₃/SnS₂ heterostructures (19.1 meV).

The VOI₂ monolayer exhibits both altermagnetism and ferroelectricity. It possesses four distinct configurations, denoted as $P \uparrow M \uparrow\downarrow$, $P \uparrow M \downarrow\uparrow$, $P \downarrow M \uparrow\downarrow$, and $P \downarrow M \downarrow\uparrow$. Here, $P \uparrow$ indicates ferroelectric polarization along the positive *a*-axis direction, while $M \uparrow\downarrow$ denotes the magnetic moments of the left (right) V atom oriented along the positive (negative) *a*-axis direction. Our calculations reveal that all four ferroelectric altermagnetic configurations are energetically degenerate. However, the alternating spin splitting varies with the direction of ferroelectric polarization and the magnetic configuration of V atoms.

The configurations $P \uparrow M \downarrow\uparrow$ and $P \downarrow M \uparrow\downarrow$ exhibit identical spin-alternating band structures, as shown in Fig. 1(d). Similarly, $P \uparrow M \uparrow\downarrow$ and $P \downarrow M \downarrow\uparrow$ display the same spin-split bands, as illustrated in Fig. 1(e). The magnitude of spin splitting in the band structure remains equal but exhibits opposite signs for the $P \uparrow M \uparrow\downarrow$ and $P \uparrow M \downarrow\uparrow$ configurations. The related spin band splitting diagram with spin orbit coupling is shown in Fig. S5 (a) and (b). This phenomenon is similar to Multiferroic Bilayer VS₂[39].

The ability to control the altermagnetic order in VOX₂

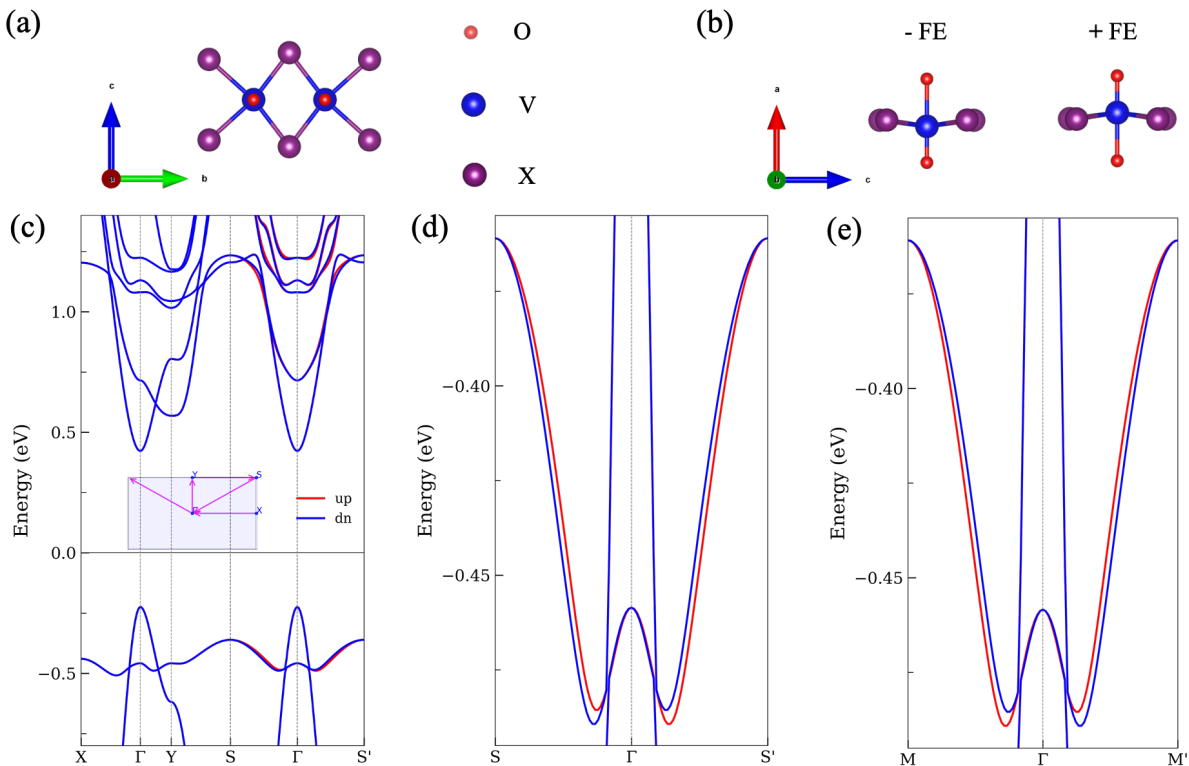


FIG. 1. (a) The side view of altermagnetic phase VOI_2 monolayer, (b) The top view of two ferroelectric directions of altermagnetic phase VOI_2 monolayer, (c) The spin-polarized band structure of VOI_2 , (d) and (e) The spin-projected valence band of negative (-FE) and positive (+FE) ferroelectric phase.

via ferroelectric polarization highlights its significant potential for next-generation high-performance electronic devices. Furthermore, the altermagnetic structure of V atoms can be switched by applying an external magnetic field [39]. By leveraging both external magnetic and electric fields, arbitrary switching among all four distinct ferroelectric interlaced magnetic states can be achieved, opening new possibilities for multistate memory applications.

MAGNETOELECTRIC COUPLING

Controlling magnetism via an electric field is one of the key challenges in next-generation information technology. To investigate the ferroelectric properties of the altermagnetic phase, we calculated the polarization of VOX_2 monolayers using the Berry phase method [40, 41]. The ferroelectric polarization of VOI_2 in the $P \downarrow M \uparrow \downarrow$ configuration along the in-plane a -axis direction is $-2.77 \times 10^{-10} \text{ C/m}$, which is close to previous calculations [34]. The corresponding polarization field is estimated as $E_P \approx 7.026 \text{ V/\AA}$ using the relation $E = P/\epsilon_0$.

To gain further insight into the ferroelectric transition, we simulated the switching pathway by linearly inter-

polating atomic positions between different ferroelectric structures. The energy barrier for the phase transition in the altermagnetic monolayer VOI_2 is calculated as 35.643 meV, as shown in Fig. 2(a). The transition barrier increases as the number of halogen elements decreases, as shown in Fig. S7. The polarization-electric field (P-E) hysteresis loop characterizes the response of ferroelectric materials to an applied electric field [42], representing a fundamental feature of ferroelectricity. Our calculations indicate a coercive field of 27.3 mV/\AA , as depicted in Fig. 2(b), demonstrating that ferroelectric polarization switching can be achieved with a relatively small external electric field.

The VOX_2 monolayer is predicted to exhibit strong magnetoelectric coupling [34]. The magnetoelectric coupling coefficient can be classified into two categories: electronic and ionic magnetoelectric coupling [33]. The variation of net magnetization with an applied electric field exhibits an approximately linear dependence, as shown in Fig. 2(c). This relationship follows the expression $\mu_0 \Delta M = \alpha_S E$ [33], where α_S is the linear magnetoelectric coupling coefficient. Here, the positive electric field is defined along the positive a -axis direction. By performing a linear fit to the data, we obtain $\alpha_S \approx 3.915 \times 10^{-7} \text{ s/m}$ for the $P \downarrow M \uparrow \downarrow$ configuration

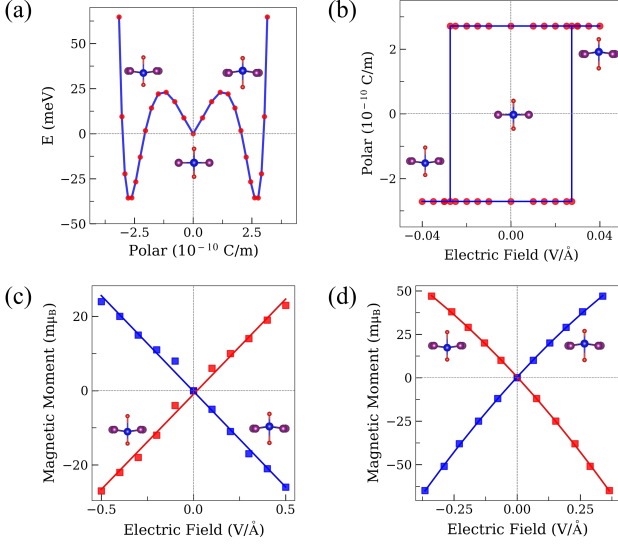


FIG. 2. (a) The relationship between polarization intensity and energy during the ferroelectric phase transition. (b) The polarization-electric field (P-E) hysteresis loop illustrating ferroelectric switching under an applied external electric field. (c) The electronic magnetoelectric coupling relationship. (d) The ionic magnetoelectric coupling relationship.

and $\alpha_S \approx -3.936 \times 10^{-7}$ s/m for the $P \uparrow M \uparrow \downarrow$ configuration.

Furthermore, during the ferroelectric phase transition, the magnetic moment undergoes a corresponding change due to the displacement of ions. The ionic magnetoelectric coupling originates from the relative positions of V ions and is closely correlated with ferroelectric polarization. Fig. 2(d) illustrates that the magnetic moment exhibits a nonlinear dependence on the applied electric field. This behavior can be numerically described by the expression $\mu_0 \Delta M = \beta_S E^2 + \alpha_S E$, where β_S represents the second-order nonlinear magnetoelectric coefficient [33]. For the $P \downarrow M \uparrow \downarrow$ configuration, we obtain $\beta_S \approx -4.494 \times 10^{-17}$ s/m and $\alpha_S \approx -1.208 \times 10^{-6}$ s/m. In the $P \uparrow M \uparrow \downarrow$ configuration, the coefficients are $\beta_S \approx -4.494 \times 10^{-17}$ s/m and $\alpha_S \approx 1.208 \times 10^{-6}$ s/m.

The VOX₂ monolayer exhibits both a substantial electronic magnetoelectric coupling effect and an unparalleled ionic magnetoelectric coupling effect. These coupling strengths are significantly larger than those observed in iron thin films ($\alpha_S^{001} = 4.35 \times 10^{-8}$ s/m) [43]. The exceptionally large magnetoelectric coupling coefficient suggests a promising avenue for electric-field control of magnetism, with potential applications in spintronics, low-power memory devices, tunable optics, and quantum computing.

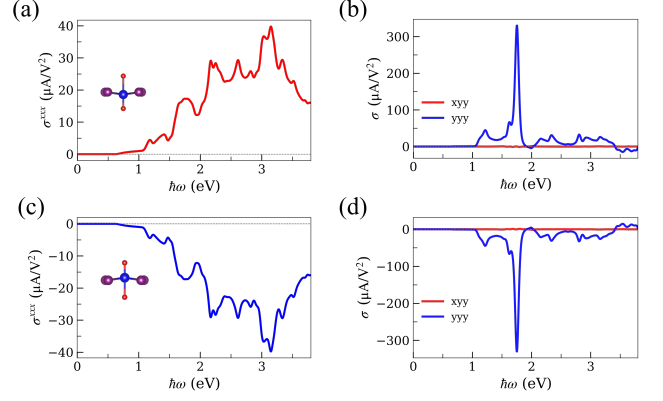


FIG. 3. (a) and (c) The σ^{xxx} component for the $P \downarrow M \uparrow \downarrow$ and $P \uparrow M \uparrow \downarrow$ configurations of VOI₂, respectively. (b) and (d) The spin SC for the $P \downarrow M \uparrow \downarrow$ and $P \uparrow M \downarrow \uparrow$ configurations of VOI₂, respectively.

SHIFT CURRENT

The absence of inversion symmetry in the VOX₂ monolayer gives rise to a SC, which is a nonlinear DC photocurrent induced by light [44–46].

Fig. 3(a) and (b) illustrate the relationship between the SC susceptibility tensor σ^{xxx} and photon energy for the VOI₂ monolayer. The σ^{xxx} component exhibits four distinct peaks in the 0–3.5 eV range. The first peak of σ^{xxx} appears at $h\omega_0 = 1.180$ eV (denoted by the lime-colored point in Fig. 3(a)), with a value of $4.443 \mu\text{A}/\text{V}^2$. This contribution primarily originates from \mathbf{k} -points near the center of the Brillouin zone (the Γ -point), as shown in Fig. S8(a). The highest peak at $h\omega_0 = 3.150$ eV exhibits a comparable magnitude of $39.775 \mu\text{A}/\text{V}^2$, arising from transitions at \mathbf{k} -points near the Brillouin zone boundary (X)(Fig. S8 (b)). This SC magnitude is comparable to that of typical two-dimensional materials, such as 2H – MoS₂ ($8 \mu\text{A}/\text{V}^2$) [47].

Moreover, noncentrosymmetric magnetic materials are known to exhibit nonlinear spin SC [48, 49]. We calculated the nonlinear spin SC in the VOI₂ monolayer, revealing exceptionally large SC magnitudes in this system. For the $P \downarrow M \uparrow \downarrow$ configuration, the σ^{yyy} component exhibits two prominent peaks at photon energies of 1.755 eV and 1.255 eV, as shown in Fig. 3(c). The largest peak occurs at 1.755 eV, reaching a substantial magnitude of $330.07 \mu\text{A}/\text{V}^2$, while the secondary peak at 1.255 eV has a value of $44.66 \mu\text{A}/\text{V}^2$. To elucidate the origin of these peaks, we analyzed the \mathbf{k} -resolved contributions of the SC. As illustrated in Fig. 4, the first peak at 1.255 eV primarily originates from electronic transitions near the Γ -point, whereas the dominant peak at 1.755 eV arises from transitions near the Brillouin zone boundary (X-point).

Furthermore, for the reversed ferroelectric polarization

configuration ($P \uparrow M \downarrow \uparrow$), the peak value of the spin SC at 1.755 eV is equal in magnitude but opposite in sign ($-330.07 \mu\text{A}/\text{V}^2$), as illustrated in Fig. 3(d). This behavior clearly demonstrates the ferroelectric tunability of the spin SC. The remarkable magnitude and switchability of both charge and spin SC highlight the potential of VOI₂ monolayers as promising candidates for nonlinear optoelectronic and optospintronic devices.

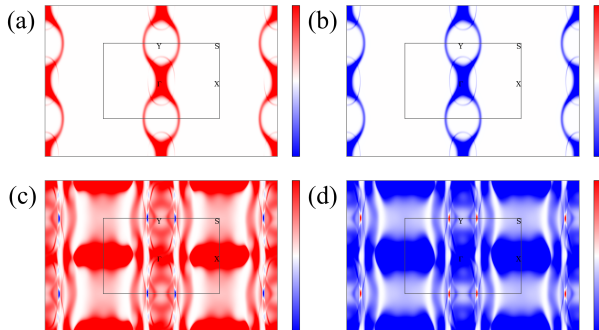


FIG. 4. (a) and (c) The distribution of spin-up SC in K space with photon energy of 1.220 eV and 1.755 eV, respectively. (b) and (d) The distribution of spin-down SC in K space with photon energy of 1.220 eV and 1.755 eV, respectively.

Since SC is a polar vector, its sign reverses upon ferroelectric polarization switching ($P_x \rightarrow -P_x$) [50]. Consequently, the sign of the SC susceptibility tensor σ^{xxx} also inverts. Thus, under the same linearly polarized light, the SC direction undergoes a 180° shift upon ferroelectric polarization switching, following the relation: $J_{\text{SC}}^{x,\leftrightarrow}(P_x) = -J_{\text{SC}}^{x,\leftrightarrow}(-P_x)$, $J_{\text{SC}}^{x,\uparrow\downarrow}(P_x) = -J_{\text{SC}}^{x,\uparrow\downarrow}(-P_x)$. Fig. 3(b) presents the SC susceptibility tensor σ^{xxx} after ferroelectric switching in the VOI₂ monolayer. The peak of σ^{xxx} remains at $h\omega_0 = 1.890$ eV, but its magnitude is equal in absolute value and opposite in sign compared to its pre-transition value ($28.00 \mu\text{A}/\text{V}^2$). This result demonstrates that external electric fields can effectively regulate SC via ferroelectric switching [51, 52]. Ferroelectric control of SC provides an excellent platform for the development of nonlinear optoelectronics in multiferroic semiconductors.

Discussion

This work investigates the unique properties of the altermagnetic phase in VOX₂ monolayers, highlighting their ferroelectric and altermagnetic multiferroic characteristics. Large quantities of oxide dichlorides MOX₂ have been studied for structural phase transitions [37, 53–55], which can break the \mathcal{PT} and $\mathcal{T}\tau$ symmetries. Altermagnetic phase may also exist in the vdW family of layered oxide dichlorides MOX₂.

The absence of inversion symmetry in these materials enables the emergence of nonlinear optical effects, such

as shift current (SC). We demonstrate that ferroelectric switching induces a 180° reversal of the SC. Other nonlinear optical effects and polar vector-related phenomena, such as injection currents, can also be driven by ferroelectricity [50].

CONCLUSION

In summary, we investigated the ferroelectric altermagnetism in VOX₂ monolayers through symmetry analysis and first-principles calculations. Our results demonstrate that VOX₂ monolayers represent a novel class of two-dimensional ferroelectric altermagnets. Further studies reveal that external fields (electric and magnetic) can reverse the band splitting, highlighting a significant magnetoelectric coupling effect. Furthermore, the nonlinear optical response, as a fundamental property of non-centrosymmetric materials, is explored. Our findings indicate that VOI₂ exhibits a pronounced SC and the SC along the x -direction can be reversed via ferroelectric control. Ferroelectric modulation of the SC presents a practical strategy for controlling nonlinear optical effects, establishing an excellent platform for exploring multiferroic semiconductors and advancing the development of high-performance optoelectronic devices. Moreover, an exceptionally large spin SC under y -direction linearly polarized light. This proves the feasibility of controlling magnetic states by electromagnetic waves in non-centrosymmetric materials and provides a new opportunity for the development of opto-spintronic applications. This work opens new avenues for investigating the interplay between ferroelectricity and altermagnetism in two-dimensional materials, laying the foundation for future innovations in energy-efficient electronics and optospintronics.

This work is supported by Shenzhen Natural Science Fund (the Stable Support Plan Program 20231121110218001), Guangdong Basic and Applied Basic Research Foundation (2022A1515012006) F. Xu also acknowledges the National Natural Science Foundation of China (Grant No. 12174262).

* jh@szu.edu.cn

- [1] L. E. Cross, Relaxor ferroelectrics, *Ferroelectrics* **76**, 241 (1987).
- [2] W. Eerenstein, N. D. Mathur, and J. F. Scott, Multiferroic and magnetoelectric materials, *Nature* **442**, 759 (2006).
- [3] M. Fiebig, T. Lottermoser, D. Meier, and M. Trassin, The evolution of multiferroics, *Nature Reviews Materials* **1**, 16046 (2016).
- [4] C. Lu, M. Wu, L. Lin, and J.-M. Liu, Single-phase multiferroics: New materials, phenomena, and physics, *National Science Review* **6**, 653 (2019).

- [5] N. A. Spaldin and R. Ramesh, Advances in magnetoelectric multiferroics, *Nature Materials* **18**, 203 (2019).
- [6] H. Yang, S. O. Valenzuela, M. Chshiev, S. Couet, B. Dieny, B. Dlubak, A. Fert, K. Garello, M. Jamet, D.-E. Jeong, K. Lee, T. Lee, M.-B. Martin, G. S. Kar, P. S  n  or, H.-J. Shin, and S. Roche, Two-dimensional materials prospects for non-volatile spintronic memories, *Nature* **606**, 663 (2022).
- [7] D. I. Khomskii, Multiferroics: Different ways to combine magnetism and ferroelectricity, *Journal of Magnetism and Magnetic Materials* **306**, 1 (2006).
- [8] K. F. Wang, J.-M. Liu, and Z. F. Ren, Multiferroicity: The coupling between magnetic and polarization orders, *Advances in Physics* **58**, 321 (2009).
- [9] J. H. Lee, L. Fang, E. Vlahos, X. Ke, Y. W. Jung, L. F. Kourkoutis, J.-W. Kim, P. J. Ryan, T. Heeg, M. Roedererath, V. Goian, M. Bernhagen, R. Uecker, P. C. Hammel, K. M. Rabe, S. Kamba, J. Schubert, J. W. Freeland, D. A. Muller, C. J. Fennie, P. Schiffer, V. Gopalan, E. Johnston-Halperin, and D. G. Schlom, A strong ferroelectric ferromagnet created by means of spin-lattice coupling, *Nature* **466**, 954 (2010).
- [10] S. Dong, H. Xiang, and E. Dagotto, Magnetoelectricity in multiferroics: A theoretical perspective, *National Science Review* **6**, 629 (2019).
- [11] V. Baltz, A. Manchon, M. Tsoi, T. Moriyama, T. Ono, and Y. Tserkovnyak, Antiferromagnetic spintronics, *Reviews of Modern Physics* **90**, 015005 (2018).
- [12] L.   mejkal, Y. Mokrousov, B. Yan, and A. H. MacDonald, Topological antiferromagnetic spintronics, *Nature Physics* **14**, 242 (2018).
- [13] D.-F. Shao and E. Y. Tsymbal, Antiferromagnetic tunnel junctions for spintronics, *npj Spintronics* **2**, 1 (2024).
- [14] H. Chen, L. Liu, X. Zhou, Z. Meng, X. Wang, Z. Duan, G. Zhao, H. Yan, P. Qin, and Z. Liu, Emerging antiferromagnets for spintronics, *Advanced Materials* **36**, 2310379 (2024).
- [15] L.   mejkal, J. Sinova, and T. Jungwirth, Beyond conventional ferromagnetism and antiferromagnetism: A phase with nonrelativistic spin and crystal rotation symmetry, *Physical Review X* **12**, 031042 (2022).
- [16] L.   mejkal, J. Sinova, and T. Jungwirth, Emerging research landscape of altermagnetism, *Physical Review X* **12**, 040501 (2022).
- [17] L. Bai, W. Feng, S. Liu, L.   mejkal, Y. Mokrousov, and Y. Yao, Altermagnetism: Exploring new frontiers in magnetism and spintronics, *Advanced Functional Materials* **n/a**, 2409327 (2024).
- [18] J. Krempask y, L.   mejkal, S. W. D’Souza, M. Hajlaoui, G. Springholz, K. Uhl řov , F. Alarab, P. C. Constantinou, V. Strocov, D. Usanov, W. R. Pudelko, R. Gonz lez-Hern ndez, A. Birk Hellenes, Z. Jansa, H. Reichlov , Z.   ob n , R. D. Gonzalez Betancourt, P. Wadley, J. Sinova, D. Kriegner, J. Min r, J. H. Dil, and T. Jungwirth, Altermagnetic lifting of kramers spin degeneracy, *Nature* **626**, 517 (2024).
- [19] S. Lee, S. Lee, S. Jung, J. Jung, D. Kim, Y. Lee, B. Seok, J. Kim, B. G. Park, L.   mejkal, C.-J. Kang, and C. Kim, Broken kramers degeneracy in altermagnetic mnte, *Physical Review Letters* **132**, 036702 (2024).
- [20] G. Yang, Z. Li, S. Yang, J. Li, H. Zheng, W. Zhu, S. Cao, W. Zhao, J. Zhang, M. Ye, Y. Song, L.-H. Hu, L. Yang, M. Shi, H. Yuan, Y. Zhang, Y. Xu, and Y. Liu, Three-dimensional mapping and electronic origin of large altermagnetic splitting near fermi level in crsb, <https://arxiv.org/abs/2405.12575v1> (2024).
- [21] J. Ding, Large band splitting in g-wave altermagnet crsb, *Physical Review Letters* **133** (2024).
- [22] R. Gonz lez-Hern ndez, L.   mejkal, K. V born y, Y. Yahagi, J. Sinova, T. Jungwirth, and J.   elezn y, Efficient electrical spin splitter based on nonrelativistic collinear antiferromagnetism, *Physical Review Letters* **126**, 127701 (2021).
- [23] L.   mejkal, Giant and tunneling magnetoresistance in unconventional collinear antiferromagnets with nonrelativistic spin-momentum coupling, *Physical Review X* **12** (2022).
- [24] Q. Cui, Y. Zhu, X. Yao, P. Cui, and H. Yang, Giant spin-hall and tunneling magnetoresistance effects based on a two-dimensional nonrelativistic antiferromagnetic metal, *Physical Review B* **108**, 024410 (2023).
- [25] K. Samanta, Tunneling magnetoresistance in magnetic tunnel junctions with a single ferromagnetic electrode, *Physical Review B* **109** (2024).
- [26] R. D. Gonzalez Betancourt, J. Zub c, R. Gonzalez-Hernandez, K. Geishendorf, Z.   ob n , G. Springholz, K. Olejnik, L.   mejkal, J. Sinova, T. Jungwirth, S. T. B. Goennenwein, A. Thomas, H. Reichlov , J.   elezn y, and D. Kriegner, Spontaneous anomalous hall effect arising from an unconventional compensated magnetic phase in a semiconductor, *Physical Review Letters* **130**, 036702 (2023).
- [27] P.-J. Guo, Z.-X. Liu, and Z.-Y. Lu, Quantum anomalous hall effect in collinear antiferromagnetism, *npj Computational Materials* **9**, 1 (2023).
- [28] K. S. Novoselov, A. K. Geim, S. V. Morozov, D. Jiang, Y. Zhang, S. V. Dubonos, I. V. Grigorieva, and A. A. Firsov, Electric field effect in atomically thin carbon films, *Science* (2004).
- [29] K. F. Mak, C. Lee, J. Hone, J. Shan, and T. F. Heinz, Atomically thin MoS_2 : A new direct-gap semiconductor, *Physical Review Letters* **105**, 136805 (2010).
- [30] L. Li, Y. Yu, G. J. Ye, Q. Ge, X. Ou, H. Wu, D. Feng, X. H. Chen, and Y. Zhang, Black phosphorus field-effect transistors, *Nature Nanotechnology* **9**, 372 (2014).
- [31] W. Sun, W. Wang, C. Yang, R. Hu, S. Yan, S. Huang, and Z. Cheng, Altermagnetism induced by sliding ferroelectricity via lattice symmetry-mediated magnetoelectric coupling, *Nano Lett.* **24**, 11179 (2024).
- [32] X. Duan, J. Zhang, Z. Zhang, I. Zutic, and T. Zhou, Antiferroelectric altermagnets: Antiferroelectricity alters magnets (2024).
- [33] C. Xu, H. Yu, J. Wang, and H. Xiang, First-principles approaches to magnetoelectric multiferroics, *Annual Review of Condensed Matter Physics* **15**, 85 (2024).
- [34] H. Tan, M. Li, H. Liu, Z. Liu, Y. Li, and W. Duan, Two-dimensional ferromagnetic-ferroelectric multiferroics in violation of the $\{d\}_0$ rule, *Physical Review B* **99**, 195434 (2019).
- [35] J. Gooth, B. Bradlyn, S. Honnali, C. Schindler, N. Kumar, J. Noky, Y. Qi, C. Shekhar, Y. Sun, Z. Wang, B. A. Bernevig, and C. Felser, Axionic charge-density wave in the weyl semimetal $(\text{TaS}_2)_2\text{Bi}$, *Nature* **575**, 315 (2019).
- [36] Y. Zhang, L.-F. Lin, A. Moreo, S. Dong, and E. Dagotto, First-principles study of the low-temperature charge density wave phase in the quasi-one-dimensional weyl chi-

- ral compound (TaSe₄), *Physical Review B* **101**, 174106 (2020).
- [37] Y. Zhang, L.-F. Lin, A. Moreo, G. Alvarez, and E. Dagotto, Peierls transition, ferroelectricity, and spin-singlet formation in monolayer *voigt*, *Physical Review B* **103**, L121114 (2021).
- [38] H. Jin, Z. Tan, Z. Gong, and J. Wang, Anomalous Hall effect in two-dimensional vanadium tetrahalogen with altermagnetic phase, *Physical Review B* **110**, 155125 (2024).
- [39] X.G. Liu, A.P. Pyatakov, and W. Ren, Magnetoelectric coupling in multiferroic bilayer *vs2*, *PHYSICAL REVIEW LETTERS* **125** (2020).
- [40] R. D. King-Smith and D. Vanderbilt, Theory of polarization of crystalline solids, *Physical Review B* **47**, 1651 (1993).
- [41] R. Resta, M. Posternak, and A. Baldereschi, Towards a quantum theory of polarization in ferroelectrics: the case of *knbo3*, *Physical Review Letters* **70**, 1010 (1993).
- [42] J. Neugebauer and M. Scheffler, Adsorbate-substrate and adsorbate-adsorbate interactions of Na and K adlayers on Al(111), *Physical Review B* **46**, 16067 (1992).
- [43] C.-G. Duan, J. P. Velev, R. F. Sabirianov, Z. Zhu, J. Chu, S. S. Jaswal, and E. Y. Tsymlal, Surface magnetoelectric effect in ferromagnetic metal films, *Physical Review Letters* **101**, 137201 (2008).
- [44] C. Wang, X. Liu, L. Kang, B.-L. Gu, Y. Xu, and W. Duan, First-principles calculation of nonlinear optical responses by Wannier interpolation, *Physical Review B* **96**, 115147 (2017).
- [45] J. Ibañez-Azpiroz, S. S. Tsirkin, and I. Souza, *Ab Initio* calculation of the shift photocurrent by Wannier interpolation, *Physical Review B* **97**, 245143 (2018).
- [46] Y. J. Zhang, T. Ideue, M. Onga, F. Qin, R. Suzuki, A. Zak, R. Tenne, J. H. Smet, and Y. Iwasa, Enhanced intrinsic photovoltaic effect in tungsten disulfide nanotubes, *Nature* **570**, 349 (2019).
- [47] A. M. Schankler, L. Gao, and A. M. Rappe, Large bulk piezophotovoltaic effect of monolayer 2H-MoS₂, *The Journal of Physical Chemistry Letters* **12**, 1244 (2021).
- [48] H. Ishizuka and M. Sato, Rectification of spin current in inversion-asymmetric magnets with linearly polarized electromagnetic waves, *Physical Review Letters* **122**, 197702 (2019).
- [49] H. Ishizuka and M. Sato, Theory for shift current of bosons: Photogalvanic spin current in ferrimagnetic and antiferromagnetic insulators, *Physical Review B* **100**, 224411 (2019).
- [50] H. Wang and X. Qian, Ferroicity-driven nonlinear photocurrent switching in time-reversal invariant ferroic materials, *Science Advances* **5**, eaav9743 (2019).
- [51] H. Wang and X. Qian, Electrically and magnetically switchable nonlinear photocurrent in *pt*-symmetric magnetic topological quantum materials, *npj Computational Materials* **6**, 199 (2020).
- [52] C. Zhang, P. Guo, and J. Zhou, Tailoring bulk photovoltaic effects in magnetic sliding ferroelectric materials, *Nano Letters* (2022).
- [53] Y. Jia, M. Zhao, G. Gou, X. C. Zeng, and J. Li, Niobium oxide dihalides NbOX₂: A new family of two-dimensional van der Waals layered materials with intrinsic ferroelectricity and antiferroelectricity, *Nanoscale Horizons* **4**, 1113 (2019).
- [54] Y. Zhang, L.-F. Lin, A. Moreo, and E. Dagotto, Orbital-selective Peierls phase in the metallic dimerized chain MoOCl₂, *Physical Review B* **104**, L060102 (2021).
- [55] Q. Guo, X.-Z. Qi, L. Zhang, M. Gao, S. Hu, W. Zhou, W. Zang, X. Zhao, J. Wang, B. Yan, M. Xu, Y.-K. Wu, G. Eda, Z. Xiao, S. A. Yang, H. Gou, Y. P. Feng, G.-C. Guo, W. Zhou, X.-F. Ren, C.-W. Qiu, S. J. Pennycook, and A. T. S. Wee, Ultrathin quantum light source with van der Waals NbOCl₂ crystal, *Nature* **613**, 53 (2023).
- [56] G. Pizzi, V. Vitale, R. Arita, S. Blügel, F. Freimuth, G. Géranton, M. Gibertini, D. Gresch, C. Johnson, T. Koretsune, J. Ibañez-Azpiroz, H. Lee, J.-M. Lihm, D. Marchand, A. Marrazzo, Y. Mokrousov, J. I. Mustafa, Y. Nohara, Y. Nomura, L. Paulatto, S. Poncé, T. Ponweiser, J. Qiao, F. Thöle, S. S. Tsirkin, M. Wierzbowska, N. Marzari, D. Vanderbilt, I. Souza, A. A. Mostofi, and J. R. Yates, Wannier90 as a community code: New features and applications, *Journal of Physics: Condensed Matter* **32**, 165902 (2020).
- [57] G. Henkelman, B. P. Uberuaga, and H. Jónsson, A climbing image nudged elastic band method for finding saddle points and minimum energy paths, *The Journal of Chemical Physics* **113**, 9901 (2000).
- [58] P. E. Blöchl, Projector augmented-wave method, *Physical Review B* **50**, 17953 (1994).
- [59] G. Kresse and J. Furthmüller, Efficiency of *ab-initio* total energy calculations for metals and semiconductors using a plane-wave basis set, *Computational Materials Science* **6**, 15 (1996).
- [60] G. Kresse and J. Furthmüller, Efficient iterative schemes for *ab initio* total-energy calculations using a plane-wave basis set, *Physical Review B* **54**, 11169 (1996).
- [61] J. P. Perdew, K. Burke, and M. Ernzerhof, Generalized gradient approximation made simple, *Physical Review Letters* **77**, 3865 (1996).